



## **Shallow retardation of the strontium isotope signal of agricultural liming - implications for isoscapes used in provenance studies**

Frei, R.; Frei, K. M.; Jessen, S.

*Published in:*  
Science of the Total Environment

*DOI:*  
[10.1016/j.scitotenv.2019.135710](https://doi.org/10.1016/j.scitotenv.2019.135710)

*Publication date:*  
2020

*Document version*  
Publisher's PDF, also known as Version of record

*Document license:*  
[CC BY](#)

*Citation for published version (APA):*  
Frei, R., Frei, K. M., & Jessen, S. (2020). Shallow retardation of the strontium isotope signal of agricultural liming - implications for isoscapes used in provenance studies. *Science of the Total Environment*, 706, [135710].  
<https://doi.org/10.1016/j.scitotenv.2019.135710>



# Shallow retardation of the strontium isotope signal of agricultural liming - implications for isoscapes used in provenance studies

R. Frei<sup>a,\*</sup>, K.M. Frei<sup>b</sup>, S. Jessen<sup>a</sup>

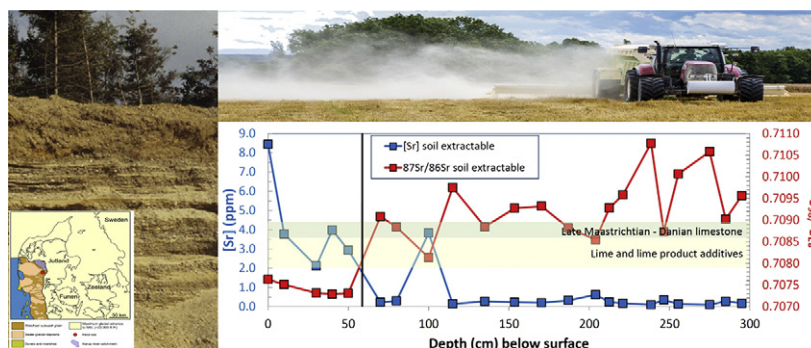
<sup>a</sup> Department of Geosciences and Natural Resource Management, University of Copenhagen, Øster Voldgade 10, 1350 Copenhagen, Denmark

<sup>b</sup> National Museum of Denmark, Department of Research, Collections and Conservation, Environmental Archaeology and Materials Science, I.C. Modewegsvej, Brede, 2800 Kgs. Lyngby, Denmark

## HIGHLIGHTS

- Agriculturally added strontium is retained in the top soils.
- We investigated a soil profile from farmland that experienced long-term liming.
- Lime-derived strontium does not penetrate into the vadose zone.
- Provenance studies depend on suitable characterization of baselines.
- Strontium in surface water is used to characterize baselines for provenance studies.

## GRAPHICAL ABSTRACT



## ARTICLE INFO

### Article history:

Received 4 September 2019

Received in revised form 21 November 2019

Accepted 21 November 2019

Available online 23 November 2019

Editor: Mae Sexauer Gustin

### Keywords:

Proveniencing

Run-off

Strontium isotopes

Biosphere

Glaciogenic sediments

## ABSTRACT

An intensified debate centers on the use of strontium isotopes in surface water run-off as archive for bioavailable signatures in prehistoric provenance studies. Its use has been challenged by a recent suggestion that modern agricultural liming of farmlands exerts a serious imprint on the strontium isotope compositions of these waters. We here present results from a soil profile beneath agricultural farmland in the glaciogenic outwash plain of central West Jutland, Denmark, which show that strontium and its isotope composition derived from lime products is efficiently retained near the surface. Pore waters and bioavailable strontium from the acidic zone below the surface soil depict strontium isotope signatures that can best be explained by a mixture of silicate-derived and relic natural (not agriculturally added) carbonate-derived strontium. We therefore argue that agricultural liming does not contaminate groundwaters and groundwater-supported surface waters, rendering reference maps based on them relevant for modern and past provenance studies.

© 2019 The Authors. Published by Elsevier B.V. This is an open access article under the CC BY-NC-ND license (<http://creativecommons.org/licenses/by-nc-nd/4.0/>).

## 1. Introduction

Isotope applications of provenance, such as used in food authenticity, counterfeit pharmaceutical characterization, illegal trade, narcotics,

wildlife migration, forensic investigations etc. (e.g., Hobson, 1999; Newton et al., 2008; van der Merwe et al., 1990; West et al., 2009), are increasingly widespread. Many of such investigations are based on the use of the isotope tracer system of strontium (Sr), which can help linking the analyzed samples of tissues or other organic substances of unknown origin to specific geographic locations. Strontium isotopes as a provenance tool is today also an integral part of prehistoric human

\* Corresponding author.

E-mail address: [robertf@ign.ku.dk](mailto:robertf@ign.ku.dk) (R. Frei).

and animal migration/mobility studies in archaeology (Bentley, 2006; Montgomery, 2010; Müller et al., 2003; Price et al., 2002). Refined methods applied to soft tissues other than tooth enamel and bone, such as wool or hair (Frei et al., 2015; Frei et al., 2017) have further contributed to high temporal resolution of prehistoric human mobility. The method is based on the fact that there is no measurable strontium isotope fractionation from geological bedrock and soil sources through the food web (Flockhart et al., 2015). Researchers involved in Sr isotope based provenance studies have become increasingly aware and sensitive of the fact that proveniencing of various animal and human tissues is substantially dependent on the delineation and adequate characterization of baselines, or isoscapes, of potential target areas. In this respect, it is imperative to concentrate on efforts to best approximate a bioavailable fraction from a geological substrate that is 1) relevant as a component transferred through the food chain, and 2) representative, in a mass budget balance, of a substantial amount of intake/diet. A variety of geological and biological materials have been investigated for this purpose (Maurer et al., 2012), but plants (Evans et al., 2010), soil extracts (Hoogewerff et al., 2019; Willmes et al., 2018) and surface waters (Frei and Frei, 2011) are currently the most widely used archives.

Surface waters have the advantage over other archives used for baseline characterizations that, if carefully selected, they represent an averaged out bioavailable signature that is usually representative for a larger target area/region, dependent of the type of reservoir sampled (usually a specific creek/river catchment area). Surface waters, in particular running and spring waters, were likely sources of Sr in the intake mass budget of prehistoric humans and certain animals. This is particularly the case in areas where carbonate sediments with usually very high Sr concentrations ( $[Sr]$ ), in the order of hundreds to thousands of ppm, rather than siliciclastic sediments with much lower  $[Sr]$ , contribute strontium to the aquifers. It is therefore expected that strontium derived from carbonates, upon entering the hydrosphere, will dominate surface run-off and groundwaters in such regions, whereby commonly more radiogenic  $^{87}Sr/^{86}Sr$  signatures mobilized from the weathering of siliciclastic sediments will be biased towards lower isotopic ratios.

Frei and Frei (2011) published a surface water-based strontium isotope reference map for Denmark (except the island of Bornholm) which is currently being used as one of the baselines for provenance studies of prehistoric humans and animals. The  $^{87}Sr/^{86}Sr$  map shows a rather homogeneous strontium isotope distribution in the surface waters (average  $^{87}Sr/^{86}Sr = 0.7096 \pm 0.0015$ ;  $2\sigma$ ;  $n = 192$ ; with a full range between 0.7079 and 0.7128), with the exception perhaps of a zone across northern Jutland where  $^{87}Sr/^{86}Sr$  values are noticeably depressed to values of 0.7079. These lower Sr isotope signatures in respective surface waters of this area seem to reflect the near-surface presence of Sr derived from Late Maastrichtian-Early Paleocene limestone/chalk, and the relative absence of the radiogenic signal of otherwise more extensive presence of Quaternary siliciclastic glaciogenic sediments covering other parts of Denmark. Upper Cretaceous-Lower Paleocene limestone and chalk in Denmark is characterized by  $^{87}Sr/^{86}Sr$  values between 0.7079 and 0.7080 (Frei and Frei, 2002; Gilleaudeau et al., 2018). Nevertheless, the strontium isotope range in surface waters reported by (Frei and Frei, 2011) is in accordance with subsequent baseline studies relying on other environmental proxy samples, such as soils, plants and fauna (e.g., Frei and Price, 2012; Frei et al., 2017; Hoogewerff et al., 2019).

This rather homogeneous distribution of Danish surface water strontium isotope composition is seen by Thomsen and Andreassen (2019) at odds with an east-west shift in  $^{87}Sr/^{86}Sr$  surface water values they expect from the distribution of natural chalk and limestone components in soils across Jutland. Strongly calcareous soils are dominant in till-dominated East Jutland, whereas low-calcareous, highly permeable and sandy Pleistocene glacial outwash sediments prevail in West Jutland (Fig. 1). These authors argue for a serious contamination of surface waters in glacial outwash plains by modern agricultural lime, in their view rendering these baselines inappropriate to reflect the water signature prior to modern agricultural liming activities. Hence, Thomsen and

Andreassen (2019) question the use of existing water-based baselines for provenance and migration studies of particularly prehistoric humans and animals. These authors take their skepticism a step further in that they postulate that this situation is common throughout recently glaciated areas along the periphery of the Weichsel and Saale ice sheets in Northern Europe.

Our study shows, however, that strontium added via agricultural liming in a representative site in the West Jutland sandy outwash plain is efficiently retained, inferably over decades, within the zone acidified in response to carbonate leaching. We infer that modern agricultural liming is not a threat to the construction of reference isoscapes in these areas when using suitable surface waters.

## 2. Materials and methods

Sediment cores were collected in March 2014, using Ø5 polyethylene liners mounted in a stainless steel tube pushed down by a jackhammer. Upon recovery the cores were immediately sealed and stored at 5 °C.

For the present study, a vertical profile of pore water was obtained by installing in December 2010 ten PRENART Super Quartz PTFE suction cells, depth-distributed vertically over the unsaturated zone and horizontally <0.5 m apart. The suction cells were beforehand equipped a septum at the upwards facing end and mounted at the tip of Ø32 mm PVC tubes with the septum inside the tube. Installation holes (Ø50mm) were made by percussion using a Geoprobe®. Before installation, 400 mL of a silica flour-water slurry was transferred to the bottom of the hole through a flexible tube and the suction cell-PVC tube assembly was then installed immediately after forming a well. This procedure ensured a good hydraulic connection for the suction cell to the pore water in the unsaturated zone sand. The small annulus around the PVC tube was afterwards filled with manufactured certified clean well pack quartz sand to 0.3 m below ground and then with top soil to the surface. Pore water from the unsaturated zone was collected ten times between May 2011 and March 2014; samples from March 2014 were used for the present work. Pore water samples were collected by lowering into the well a pre-evacuated septum glass contained in a shuttle with the septum facing downwards. The shuttle held at its lower end a spring-mechanism with a double-ended needle. Upon unification between the shuttle and the septum of the suction cell, the needle ensured hydraulic contact between the unsaturated zone pore water and the evacuated inner of the septum glass. After 24 h the shuttle holding the septum glass was retrieved, and the septum glass was removed and stored at 5 °C. The profile was further equipped with a piezometer at 6.5 m below surface, installed in a similar way as the suction cells, to enable monitoring of the groundwater water table elevation and sampling of saturated zone using a peristaltic pump. Pore waters collected in septum glasses were transferred to 20 mL polyethylene vials through 0.21 µm cellulose acetate syringe filters (Sartorius Minisart) following the fieldwork in March 2014 and stored at 5 °C. For the present study, volumes of 1–2 mL of these pore water samples were analyzed for their strontium isotope signatures, and some samples also for their  $[Sr]$ . One sample collected from the groundwater table at c. 6.6 m depth was also analyzed. Concentrations reported for these water samples refer directly to those in the waters.

Subsamples of the core (surface to −3.0 m below terrane level, samples A-H; 1–14) were sieved to <2 mm (Fig. S1), and aliquots of 10 g were exposed to 25 mL of ultrapure 1 M ammonium nitrate solution in 50 mL centrifuge tubes for two hours during which the tubes were tumbled feebly. We adhered to the recipe applied for the provenance-suitable isoscape reference maps of France and Europe by (Hoogewerff et al., 2019; Willmes et al., 2018), and elsewhere, to recover a relevant bioavailable fraction of strontium from soil sediments. After centrifugation, 5 mL aliquots of these solutions were used to determine the strontium isotope composition (IC), 2 mL aliquots were spiked with a  $^{84}Sr$  enriched tracer solution to determine the strontium

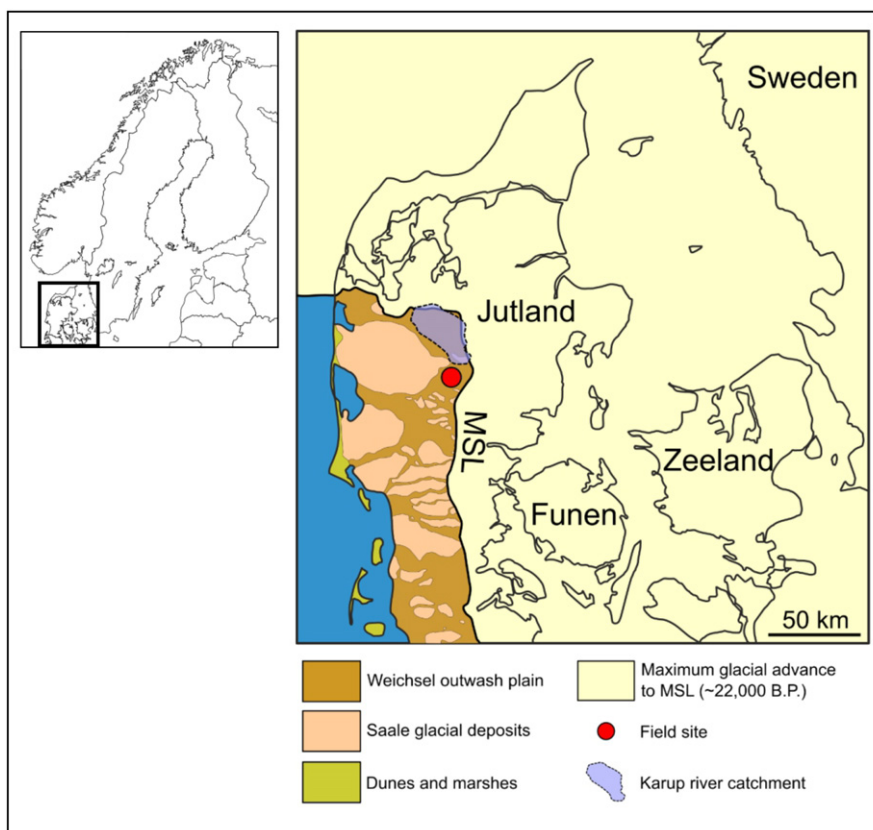


**Fig. 1.** Landscape geomorphological map of Jutland, Denmark. Map showing the distribution of periglacial and post glacial sediments related to the Saalian and Weichselian glaciations on the Jutland peninsula. Western Jutland is dominated by outwash plain sediments. The site of the profile studied herein is marked with a red dot and the approximate area of the Karup river catchment is outlined by the blue shaded area (see legend). Dark blue area indicates sea and brackish lagoons. The Main Stationary Line (MSL), separating West and Central Jutland, marks the maximum extent of the Scandinavian ice sheet during the last Glaciation (22'000 B.P.). Modified from (Greve et al., 2012). The inset shows the study area in Denmark in relation to Scandinavia.

concentration [Sr] via isotope dilution (ID), and 2 mL were used for major and trace element concentrations measured by ICP-MS. In addition, five sieved core samples weighing one gram each were attacked by 10 mL of *aqua regia* for 24 h on a hotplate. Finally, we performed 0.2 M acetic acid leaches on 1 g amounts of five <2 mm soil sample aliquots in order to preferentially attack relic detrital carbonates. For this, we exposed the samples to 10 mL of 0.2 M acetic acid for 30 min under tumbling at room temperature, and separated strontium from 1 mL aliquots of the leachates after adding a  $^{84}\text{Sr}$  enriched spike. Concentrations of the respective ammonium nitrate, acetic acid leachates and *aqua regia* extracts are expressed relative to the <2 mm sample weights processed.

For strontium isotope measurements, including spiked samples for ID analyses, respective leachates were dried on a hotplate in Savillex Teflon beakers, after which the residues were taken up in 3 M  $\text{HNO}_3$  and passed over miniaturized extraction columns (1 mL disposable pipette tips fitted with a porous frit) charged with 300  $\mu\text{L}$  of 100 mesh SrSpec<sup>TM</sup> (Triskem) resin. After flushing with 4 mL of 3 M  $\text{HNO}_3$ , strontium was released from the resin with 2 mL of ultrapure water. Strontium separates were loaded onto outgassed rhenium filaments in 2.5  $\mu\text{L}$  of a mixed  $\text{Ta}_2\text{O}_5$ - $\text{H}_3\text{PO}_4$ -silica gel mixture and measured dynamically on a VG sector 54 IT thermal ionization mass spectrometer. Mass fractionation was controlled by  $^{86}\text{Sr}/^{88}\text{Sr} = 0.1194$  for IC analyses, and deconvolution of spiked samples was performed externally for the ID samples. 50 ng loads of the NBS 987 Sr standard gave  $^{87}\text{Sr}/^{86}\text{Sr} = 0.710238 \pm 0.000020$  ( $n = 5, 2\sigma$ ). The  $^{87}\text{Sr}/^{86}\text{Sr}$  values of the samples were corrected for the offset relative to the NIST SRM 987 value of 0.710245 (Thirlwall, 1991). Procedural strontium blanks remained below 200 pg with an average  $^{87}\text{Sr}/^{86}\text{Sr}$  value of  $-0.709$ , an amount which is insignificant relative to the >60 ng of sample strontium

processed and thus did not require correction of the measured strontium isotope signatures for blank contribution.

For major element concentration analyses by ICP-MS, the dried down ammonium nitrate aliquots were re-dissolved into 10 mL of a 1 vol%  $\text{HNO}_3$ . These solutions were measured with a Perkin Elmer ELAN 6000 quadrupole ICP-MS at the Geological Survey of Denmark and Greenland (GEUS), following procedures and respective standard controls described by Kystol and Larsen (1999).

### 3. Results

We studied the first ~3 m of a multi-level profile through a ~5 m thick sandy unsaturated zone of an agricultural field, 10 km south of the town of Ikast, Denmark (Fig. 1, 56°02'06"N, 9°10'24"E, 67 m a.s.l.). The site lies within the sandy Quaternary glacial outwash sediments that dominate the western part of the Jutland peninsula (Denmark) and was referred to by Thomsen and Andreasen (2019) as the West Jutland glaciogenic province (Fig. 1). The outwash sand, as is frequently the case (Böhlke et al., 2002; Postma et al., 1991; Robertson et al., 1996), was originally co-deposited with fragments of pre-Quaternary carbonates derived from the ice sheets' erosional source area. However, acid soils and heath vegetation subsequently developed due to carbonate leaching (Friborg, 1996; Odgaard and Rasmussen, 2000; Reardon et al., 1979). Agriculture in the outwash plain is therefore extremely difficult and reliant on agricultural liming which in West Jutland began at the end of the 1800s. The site studied herein appears as farmland on maps dating back to at least 1913. Liming at the site therefore probably was initiated a few decades into the 1900s, and likely became routine agricultural practice in the middle of the 1900s.



Samples of pore water and push core sediments throughout the unsaturated zone were obtained from the site. Pore water from the four multi-level profiles at the site show a marked pH decrease within the unsaturated zone, from 6 to 6.5 in the upper parts to <5 in the lower part, paralleled by a complete loss of ~1 meq/L alkalinity at the depth of the pH shift (Jessen et al., 2014; Thaysen et al., 2014). The acidic sub-soil reflects the post-Pleistocene carbonate leaching and soil acidification in West Jutland outwash plains, whereas the upper near-neutral pH reflects the effect of agricultural lime addition.

### 3.1. Bioavailable strontium concentrations and isotope compositions

Results of strontium isotope signatures and [Sr] from leachates of the push core samples, pore waters and the groundwater are listed in

Table S1. The double y-axis plot in Fig. 2A displays the sediment [Sr] and  $^{87}\text{Sr}/^{86}\text{Sr}$  that were measured in ammonium nitrate leachates (henceforth referred to as bioavailable Sr). [Sr] in the top ~60 cm of the profile range from 2.1 to 8.4 ppm, and [Sr] decreases abruptly to much lower concentrations in the range from ~0.10 to 0.61 ppm in the deeper part of the profile. An opposite trend is expressed by the  $^{87}\text{Sr}/^{86}\text{Sr}$  signatures, with a narrow band of 0.7073 to 0.7076 in the top 60 cm of the profile, and more heterogeneous but elevated signatures between ~0.7081 to 0.7105 in the deeper parts of the profile. Quite clearly, the upper c. 60 cm of the soil profile is dominated by Sr derived from the agriculturally added lime, because lime products used in Denmark are characterized by elevated [Sr], and  $^{87}\text{Sr}/^{86}\text{Sr}$  values ranging from 0.7075 to 0.7079 (Thomsen and Andreassen, 2019). The changes in both [Sr] and  $^{87}\text{Sr}/^{86}\text{Sr}$  values below 60 cm depth are

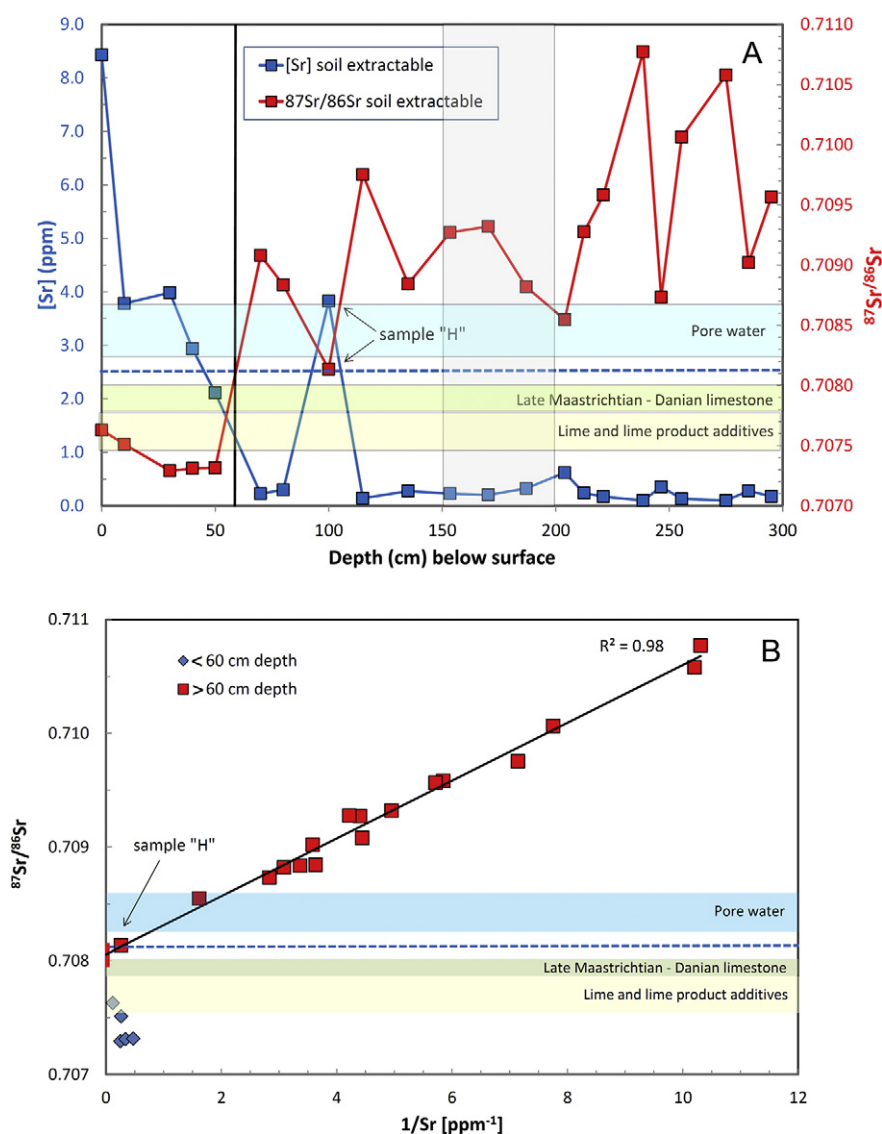


**Fig. 2.** Bioavailable strontium concentrations and strontium isotope compositions in the soil profile. A. Double y-axis diagram with [Sr] (blue symbols) and  $^{87}\text{Sr}/^{86}\text{Sr}$  values (red symbols) plotted against profile depth. A defined jump towards lower [Sr] and higher  $^{87}\text{Sr}/^{86}\text{Sr}$  value occurs at around 60 cm depth (marked with black vertical line), separating Sr associated with agricultural lime above this barrier from Sr from weathering siliciclastics and natural relic detrital carbonates below. The transparently colored bands represent the  $^{87}\text{Sr}/^{86}\text{Sr}$  value range of lime and lime product additives ((Thomsen and Andreassen, 2019); pale yellow), of Late Maastrichtian-Danian limestones ((Frei and Frei, 2002; Gilleaudeau et al., 2018); pale green) and of pore waters from the soil profile measured herein (pale blue). The  $^{87}\text{Sr}/^{86}\text{Sr}$  value of the groundwater at 6.6 m depth is indicated by a blue dashed line. Sample "H" from 1 m depth closely depicts the isotope composition of relic detrital carbonates found in this particular sample. B. Mixing diagram showing the relationship between  $1/\text{[Sr]}$  and  $^{87}\text{Sr}/^{86}\text{Sr}$  values in samples of the soil profile. Samples from below 60 cm depth (red symbols) define a well constrained two source endmember mixing array ( $R^2 = 0.98$ ) with unradiogenic Sr from natural relic detrital carbonates and radiogenic Sr derived from the weathering silicates in the lower part of the profile. The red-filled rectangle centered around the intersection of the mixing line with the y-axis depicts the  $^{87}\text{Sr}/^{86}\text{Sr}$  compositional range of the relic detrital carbonate endmember. Sr in the upper 60 cm of the profile (samples in blue symbols), depicting the Sr from agricultural lime additives, is unrelated from the signatures in the lower parts, implying its efficient retardation in the topsoils. Transparent bands and the blue dashed line are the same as in A. For details refer to text.

important to the understanding of the effect of agricultural lime addition in surface waters. In Fig. 2B we present a mixing diagram in form of  $1/[Sr]$  vs.  $^{87}Sr/^{86}Sr$  for the bioavailable fraction recovered from the core segments by ammonium nitrate. Linear relationships in such a diagram express two-component mixtures. In this diagram it becomes clear that samples above c. 60 cm are decoupled from samples below this depth. Below 60 cm the samples define a very well characterized linear relationship ( $R^2 = 0.98$ ), with one endmember being characterized by high  $[Sr]$  and a  $^{87}Sr/^{86}Sr$  ratio of  $0.70805 \pm 0.00010$  ( $2\sigma$ ) (defined by the extrapolated intersection value of the mixing line with the y-axis), and the other endmember being characterized by low  $[Sr]$  but elevated strontium isotope ratios, closely matching the surface waters from the Central and West Jutland glaciogenic province which Thomsen and Andreassen (2019) classified as being agriculturally overprinted. We equate the first of the former endmembers with bioavailable Sr derived from small amounts of relic detrital carbonates present in the lower portion of the profile, and the second endmember

with radiogenic Sr derived from the weathering of the predominant clastic silicates, unaffected by Sr from the agricultural liming products. Our interpretation is supported by the silicate-dominated  $^{87}Sr/^{86}Sr$  signatures (range 0.7091–0.7269,  $n = 5$ ) obtained from *aqua regia* soil attacks, and the relic-carbonate's isotope signature (range 0.7083–0.7086,  $n = 5$ ) approached by weak acetic acid leachates (Table S1).

An important observation in Fig. 2B is, that the isotope signature of the samples above 60 cm is significantly lower than the relic carbonate endmember, meaning that the high  $[Sr]$ -low  $^{87}Sr/^{86}Sr$  sources being tapped by the ammonium nitrate leaching procedure are different. The first one, present above 60 cm depth and with  $^{87}Sr/^{86}Sr$  in the range 0.7075–0.7076, reflects the agriculturally added lime products. However, the second one, present below 60 cm depth and with  $^{87}Sr/^{86}Sr$  in the range 0.7081–0.7115, we equate with relic likely Late Maastrichtian-Early Paleocene carbonate components disseminated in the sandy glaciogenic and predominantly siliciclastic sediment (Fig. S1). Sample "H" with the highest  $[Sr]$  and lowest  $^{87}Sr/^{86}Sr$  ratio

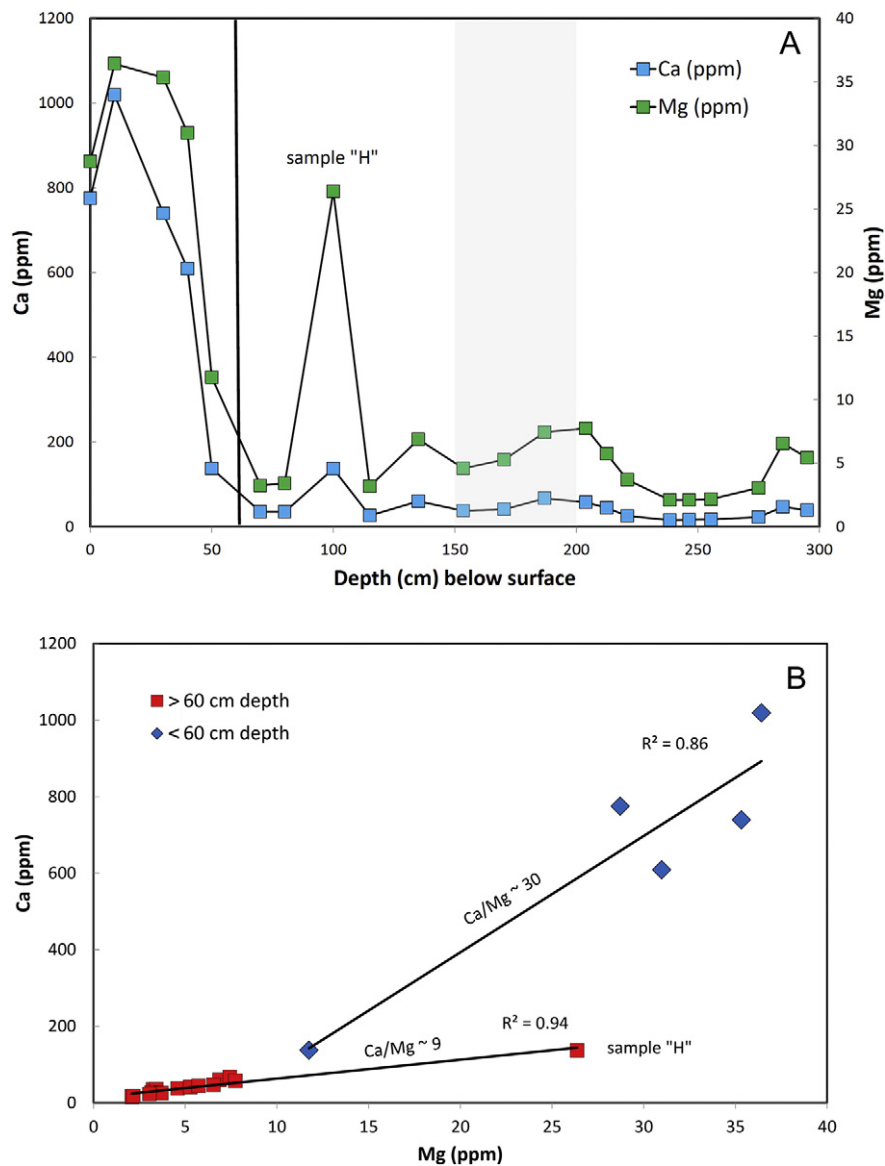


**Fig. 3.** Major element relationships in the soil profile. A. Concentrations of bioavailable Ca (blue symbols) and Mg (green symbols) of soil samples versus sampling depth. Both major elements are strongly concentrated in the top 60 cm (barrier marked with a black vertical line), compared to low concentrations of these elements in the deeper parts of the profile. The grey shaded vertical area marks the zone where there is a pronounced shift in pH from values around 7 above to 5–6 below the transition zone. Sample "H" from 1 m depth is dominated by contribution of these elements from relic detrital carbonates. B. Scatterplot depicting the relationship between  $[Mg]$  and  $[Ca]$  in bioavailable soil extracts from the profile studied. Samples from above 60 cm depth are distinguished from samples below 60 cm, both in their overall concentration ranges and in the  $Ca/Mg$  ratios (reflected by the slopes of the respective correlation lines). For details refer to text.

(Table S1; Fig. 2A) very closely approximates this source. Mass balance calculations predict that only a very small amount of such relic carbonate in a traditionally classified “non-calcareous” glaciogenic outwash sediment is necessary to lower the radiogenic bioavailable strontium fraction of the sedimentary clastic silicates. A simple calculation reveals that only ~0.2% of a predominantly limestone or chalk derived bioavailable component with [Sr] typically around 5 ppm and a  $^{87}\text{Sr}/^{86}\text{Sr}$  signature of 0.708 is necessary to lower a silicate-derived component (with 0.2 ppm [Sr] and a  $^{87}\text{Sr}/^{86}\text{Sr}$  value of 0.730), to a signature of 0.7084 typical of the measured pore water composition (Table S1). This shows the extreme sensitivity of the isotope composition of bioavailable strontium in sandy soils typical of originally calcareous glacial moraines and outwash sediments, and asks for caution in properly addressing and isolating this component for provenance-oriented studies.

### 3.2. Selected major element compositions in leachates

Bioavailable major element concentrations, as measured by ICP-MS in filtered ammonium nitrate leachate aliquots expressed relative to the weight of the treated <2 mm grain size soil fraction, are contained in Table S2. The concentration profiles of Ca and Mg, shown in Fig. 3A, follow that depicted by [Sr] (Fig. 2A). [Ca] and [Mg] exceeding 600 ppm and 20 ppm, respectively, are characteristic of samples above 50 cm, while concentrations generally lower than 200 ppm and 12 ppm, respectively, are measured below 50 cm depth (Fig. 3A). The elevated bioavailable (mobile) [Ca] and [Mg] are due to the addition of agricultural chalk and magnesium chalk, but like in the case of Sr, these elements are efficiently retained near the surface and do not penetrate significantly into the lower part of the profile. In Fig. 3B, depicting [Ca] vs. [Mg] (Table S2), samples from below 60 cm depth define a flat and well defined linear relationship ( $R^2 = 0.94$ ). This suggests a proportionate partitioning of these elements into the leachate characterized by bioavailable Ca/Mg of ~9 (Fig. 3B). It also implies a rather homogenized release of these elements, which attests for the presence of one predominant source for Ca and Mg. We note that sample “H” from 1 m depth with the highest [Ca] and [Mg] (Fig. 3A) best approximates the Sr composition of the relic carbonate fragments (Fig. 3B). While sample “H” exhibits Sr and Ca concentrations that are similar to those of samples from

the top 60 cm of the profile, it is the Ca/Mg ratio of this sample that fits to the flat-lying trend depicted in Fig. 3A and thus matches the released major element characteristics of relic carbonates in the lower part of the soil profile. The samples from the top 50 cm of the profile have substantially higher [Ca] and [Mg] with, at average, a much higher Ca/Mg of ~30 defined by the slope of the regression line ( $R^2 = 0.86$ ; Fig. 3B). Together, these results strongly imply the existence of a retardation front around 60 cm depth at which an efficient inhibition for the transfer of cations from agricultural lime products down into the vadose zone occurs.

In order to explore the process inhibiting the downwards transfer of base cations, including  $\text{Sr}^{2+}$ , we inspect the behavior of bioavailable aluminum (Al) in the profile (Fig. 4). Concentrations of bioavailable Al are below 10 ppm in the upper 1 m of the profile and then increase downwards approaching ca. 50 ppm (Fig. 4). This somewhat opposite behavior of Al relative to that of Ca and Mg (Fig. 3A) is observed also in other studies of sandy glaciogenic soil profiles (Hansen and Postma, 1995), and reflects the tendency of down-transported  $\text{Al}^{3+}$ , released as a result of post-glacial soil acidification in the outwash plain prior to modern agricultural liming, to displace adsorbed base cations including  $\text{Ca}^{2+}$  and  $\text{Mg}^{2+}$  from cation exchange sites (Lindsay, 1979). The low [Al] in the upper part of the profile reflects the effects of lime addition and the consequent displacement of Al by Ca and Mg. Liming, in this way, has decreased the acidity associated to Al (also termed the aluminum toxicity) and enabled the increased pore water pH and alkalinity, as observed in the upper part of the profile by Jessen et al. (2014). Likewise, our results from dissolved Si in some of the pore waters ([Si] plotted in Fig. 4 along with [Al]) speak for an increased mobility of Si with the acidic zone (deeper than 2 m depth; Jessen et al. (2014)). This indicates acid-promoted enhanced weathering of the silicates, which is similarly reflected by the overall elevated  $^{87}\text{Sr}/^{86}\text{Sr}$  values of bioavailable Sr fractions in this deeper part of the profile (Fig. 2A).

### 4. Discussion

Thomsen and Andreassen (2019) cast doubts on the use of existing surface water-based isoscapes from agriculturally limed areas characterized by low- to non-calcareous soils, which typically are a result of the weathering of glacial outwash plain sediments. Outwash plains

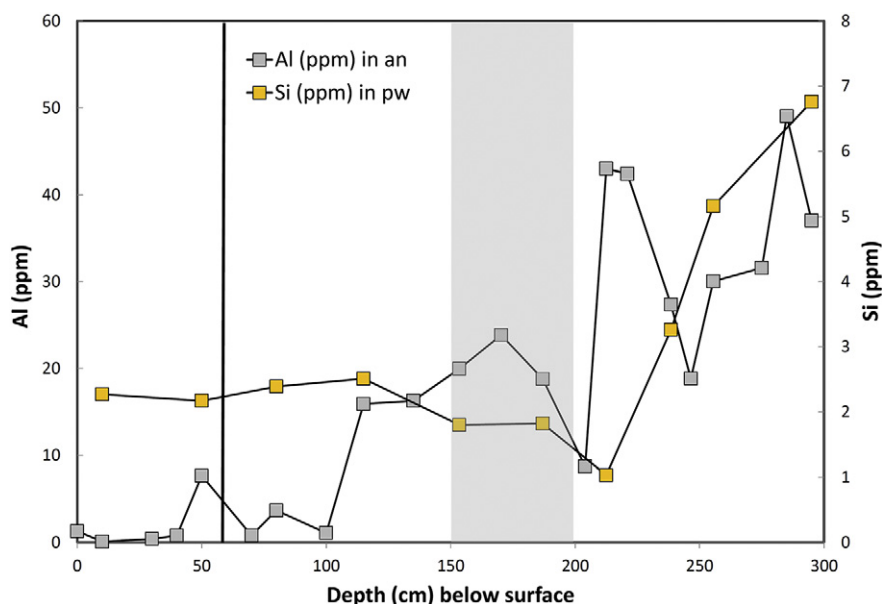


**Fig. 4.** Aluminum and silicon relationships in the soil samples and pore waters. Diagram showing soil bioavailable [Al] (grey symbols) and [Si] (yellow symbols) in pore waters plotted against profile depth. The generally increasing [Al] with depth indicates increased acid-promoted weathering of siliciclastics. [Al] in the topsoil (cation transfer barrier marked with a black vertical line) is low because of competition for cation adsorption sites by  $\text{Ca}^{2+}$  and  $\text{Mg}^{2+}$  added by lime product additives. Below the zone characterized by a marked decrease in pH (marked by grey shaded area), an increased mobility of Al is also noted in the respective pore waters. For discussion refer to text.

frequently occur in the periglacial landscapes of the northern hemisphere. These authors infer that today all larger lakes, most streams, and all rivers in such areas are affected by agricultural liming, so that the modern prevailing strontium isotope signatures used for baseline maps do not reflect the bioavailable signatures that prevailed in prehistoric times. Our results presented herein argue against this generalization and the postulation that lime product-derived strontium contaminates the run-off in respective catchments within the glacial outwash plains of West Jutland.

First, the effective retention of Sr added by lime products in the topsoil, illustrated in Fig. 2A, shows that lime product-derived strontium and its isotope signature in practice does not enter the vadose zone and underlying aquifer, to ultimately discharge to surface water and in this way substantially alter the isotope signature of the natural bioavailable strontium that constituted the intake for prehistoric humans and animals. The mixing relationships depicted in Fig. 2B show a clear spatial separation between the uppermost c. 60 cm of the profile and the lower part, with respect to strontium isotope signatures in the bioavailable fractions. While the  $^{87}\text{Sr}/^{86}\text{Sr}$  of bioavailable Sr above 60 cm depth ( $^{87}\text{Sr}/^{86}\text{Sr} = 0.7072\text{--}0.7076$ ) is compatible with Sr from lime products ( $^{87}\text{Sr}/^{86}\text{Sr} = 0.7075\text{--}0.7079$ ; Thomsen and Andreassen (2019)), the isotopic signature of bioavailable Sr below 60 cm depth is not. Instead the values are more radiogenic ( $^{87}\text{Sr}/^{86}\text{Sr} = 0.7082\text{--}0.7115$ ). The mixing relationship depicted by leachates from below 60 cm imply a derivation of Sr from siliciclastics with elevated  $^{87}\text{Sr}/^{86}\text{Sr}$  ratios (Table S1), but, most importantly, also from a pool of Sr stored in the subsoil, which releases higher [Sr] with lower  $^{87}\text{Sr}/^{86}\text{Sr}$ . This Sr may be stored in an adsorbed form, or perhaps as a small amount of natural relic detrital carbonates ( $^{87}\text{Sr}/^{86}\text{Sr} \sim 0.70805$ ). Nonetheless, it becomes evident that the bioavailable fractions that enter the vadose zone are dominated by Sr matching relic detrital carbonates, which are set to depress the radiogenic, but low [Sr] component from the siliciclastics ( $^{87}\text{Sr}/^{86}\text{Sr} > 0.7108$ ). Here it is important to notice that surface waters and groundwaters are especially closely linked in permeable settings of an outwash plain. Aquifer recharge takes place in most of the sandy outwash plain area, while discharge to surface waters is limited mostly to stream valleys. Therefore, aquifer flow paths that enter deeper still-calcareous zones of the aquifer inevitably will constitute a part of the flow paths which converge to form the discharge of regional surface water rivers and streams. According to these hydrogeological considerations, running surface waters will in any case acquire an imprint of the [Sr] and isotope signature of the detrital relic carbonates of the outwash plain aquifers. Therefore surface waters in general, and also in areas dominated by glaciogenic outwash sediments, are characterized by a relatively narrow range of low

$^{87}\text{Sr}/^{86}\text{Sr}$  values between 0.7079 and 0.7128 (average  $0.7096 \pm 0.0015$ ;  $2\sigma$ ,  $n = 192$ ) defined in the study of Frei and Frei (2011).

The Karup river catchment, located within the outwash plain, is interpreted by Thomsen and Andreassen (2019) as a representative case for the contamination of surface water by Sr derived from the modern addition of lime products. Indeed, increasing [Sr] and decreasing  $^{87}\text{Sr}/^{86}\text{Sr}$  values are observed along Vallerbæk brook, a brook in the catchment, as its course exits a pristine area and enters an agricultural area. The authors note that Vallerbæk brook's discharge, when the brook runs within the pristine area, must be based on surface water as the groundwater table is below the level of the brook. Only when Vallerbæk brook enters the agricultural area it may begin to receive groundwater (Thomsen and Andreassen, 2019). In line with the above hydrogeological considerations, the increasing [Sr] and decreasing  $^{87}\text{Sr}/^{86}\text{Sr}$  values, observed by Thomsen and Andreassen (2019) as Vallerbæk brook enters the agricultural area, could therefore as well result from discharging deep flow paths carrying a Sr imprint from detrital relic carbonates and hence need not to be associated to the change in land use along the brook. A generic conceptual hydrogeological model which fits the situation described by Thomsen and Andreassen (2019) for Vallerbæk brook and the Karup river catchment is illustrated in Fig. 5 which will be discussed below.

#### 4.1. Mechanisms of Sr signal retention

Our results show the effective retention of the isotope signature of agricultural lime-derived Sr, and therefore speak against water signatures in streams and lakes as being significantly affected by agricultural lime-contaminated near-surface run-off within the outwash plain. We observed the Sr retention front at just 60 cm depth, within previously acidified soil horizons. As mentioned, the Sr signature below this depth is distinctly different from the Sr signature above 60 cm depth and matches that of the detrital carbonates. Because of the latter, we suggest that relic detrital carbonates, even in sediments often classified as non-calcareous in the area of western Jutland, play a role. In our case, this is supported also by the fact that fragments of detrital carbonates were observed in our sediment samples (Fig. S1). In the case of Vallerbæk brook, a detrital carbonate content, significant enough to control the major ions groundwater chemistry at 15 m below the groundwater table, exists within the outwash plain sediments of the Karup river catchment (Postma et al., 1991). By their dissolution these carbonates immediately must be expected to directly imprint groundwater discharging to the downstream end of Vallerbæk brook and to

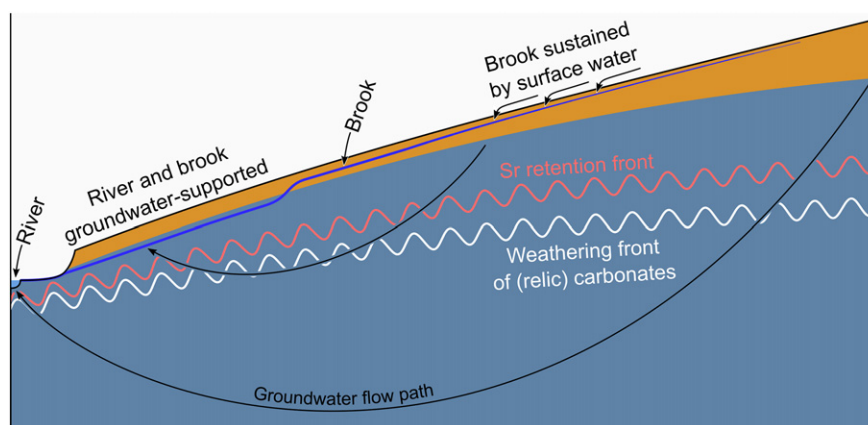


**Fig. 5.** Conceptual hydrogeological model. The sketch displays the elevation of the groundwater table (blueish area) relative to that of the terrain (orange), a brook (blue line), and the connected downstream river. The discharge of brooks and (more regional) streams and rivers in the outwash plain are variably sustained by groundwater. The Sr retention front and the weathering front of (relic) detrital carbonates are displayed individually. Groundwater acquires the Sr signature matching detrital carbonates when it crosses the Sr retention front or the carbonate weathering front, and carries this signal to the recipient surface water body.



Karup river with the Sr isotope signature significantly controlled by detrital carbonates.

However, the shallow Sr retention front observed in our data contrasts with data of Thomsen and Andreasen (2019) who measured radiogenic  $^{87}\text{Sr}/^{86}\text{Sr}$  values at c. 10 m below the groundwater table in two wells (their KG-2 and KG-3 samples) sampling acidic groundwater. This suggests much deeper positions of the Sr retention front and the weathering front of relic detrital carbonates at their location. Furthermore, the opposite trends of the [Ca] and [Mg] profiles vs. the [Al] profile (Figs. 3A and 4), we interpret as being most likely a result of cation exchange. In that case also the mechanisms for Sr and  $^{87}\text{Sr}/^{86}\text{Sr}$  retention are linked to cation exchange, as the Ca and Sr behave quite alike during cation exchange. This infers a process for the Sr retention by which the existence of relic detrital carbonates would not be necessary, as long as the Sr released from their weathering would accumulate to an (adsorbed) pool in the sediment. It is obvious from the profile studied that the Sr retention level roughly corresponds with the occurrence of darker, organic material-enriched soils in the top part (samples A-D; Fig. S1). The role of organic matter functional groups in the adsorption of Sr in wetlands has recently been studied by Boyer et al. (2018). Their study revealed high to very high, and mostly poorly reversible, Sr adsorption onto all wetland organic substrates, despite acidic pH <5 typically prevailing in such environments. Large Sr adsorption capacities were also found in wetland sediments, and these authors attributed them to the occurrence of natural clays, organic molecules, and the large fraction of carbon found in proteins. Boyer et al. (2018) propose therefore engineered organic components in wetlands as means to efficiently delay Sr transport towards downstream surface ecosystems, and consequently an effective means to manage radioactive  $^{90}\text{Sr}$  pollution. Such a scenario would explain the effective retention over decades, in the upper soil layers, of agriculturally added Sr via liming to respective farmland, as revealed by the studied profile herein.

Our combined interpretation is accordingly open towards a decoupling of the two fronts, and Fig. 5 thus displays separate fronts for the Sr retention and for the weathering of (relic) detrital carbonates. In Fig. 5 the Sr retention front is placed at below the groundwater table (i.e., at significant depth below the soil) to be consistent with both Thomsen and Andreasen (2019)'s and our own data, and above the weathering front for (relic) detrital carbonates to indicate the possible separation of the two. Its lowest possible position must coincide with the uppermost position of relic carbonates. In generic form, Fig. 5 suggests that streams in outwash plain sediments may or may not receive groundwater discharge depending on the elevation of the stream relative to that of the groundwater table. Groundwater that follows deeper flow paths acquire the Sr signal matching detrital carbonates as it crosses the Sr retention front or enter calcareous strata in the aquifer. Still calcareous sediments are expected to be closer to the surface near rivers than in the recharge area of a catchment because at least a fraction of the discharging flow paths have already approached calcite saturation up-gradient to the point of discharge.

#### 4.2. Mass balance calculation

According to Thomsen and Andreasen (2019), the agricultural lime product applied in Jutland today consists of a mixture of Upper Cretaceous chalk from northern Jutland and Permian Magnesian Limestone imported from England. The  $^{87}\text{Sr}/^{86}\text{Sr}$  ratio of the mixture is ~0.70785, and the strontium concentration is ~800 ppm (Table S4 in Thomsen and Andreasen (2019)). This data is fully compatible with [Sr] and  $^{87}\text{Sr}/^{86}\text{Sr}$  signatures measured in Upper Maastrichtian-Lower Danian (Pliocene) chalk (Frei and Frei, 2002; Gilleaudeau et al., 2018). The [Sr] profile in Fig. 2A shows high [Sr] of 2–8.5 ppm above 60 cm depth, indicating an accumulation of the added Sr in the top of our

studied profile. Using typical average lime application rates of ~900 kg/ha/yr reported for two farms in the Vallerbæk area (Table S4; Thomsen and Andreasen (2019)) and Sr contents of 800 ppm for agricultural lime, we derive that about 720 g Sr/ha/yr is added to arable farmland typical of western Jutland. We estimate the mass of bioavailable Sr currently accumulated in the top 60 cm soil horizon, using the avg. [Sr] of ~4 ppm and a bulk density of 1.5 kg/dm<sup>3</sup> (Thaysen et al., 2014), to about 36'000 g Sr/ha. Division of this amount by 720 g Sr/ha/yr yields a time period of ~50 years, which is very compatible with the expected period of routine agricultural liming at the site. Our calculations therefore support the efficient retention of Sr from the agricultural lime products in the topsoil.

We also calculated a Sr mass balance on the Karup River catchment in western Jutland, which Thomsen and Andreasen (2019) interpret as a representative case study for the contamination by Sr derived from the modern addition of lime products. In our calculation we consider the situation at the Hagebro location of Thomsen and Andreasen (2019), where average discharge of Karup river is 6.8 m<sup>3</sup>/s derived from a catchment area of 480 km<sup>2</sup> (Thomsen and Andreasen, 2019). Assuming an agricultural strontium addition rate of 720 g Sr/ha/yr (Thomsen and Andreasen, 2019) to respective farmlands that is "dissolved at a rate corresponding to its yearly supply" (Thomsen and Andreasen, 2019), and estimating the catchment to be covered by 80% arable land (judged from satellite imagery), we calculate that the average [Sr] in the catchment head water of the Karup River should be about 0.13 mg/L. This is c. 20% higher than the concentration actually measured by the authors (i.e. 0.11 mg/L). This seems to imply that agricultural lime-derived Sr is not fully transferred into the surface water but instead is at least partially retained in the farmland soils of this catchment. Much more importantly, if a significant portion of the Sr in the Karup river would be due to agricultural lime-based Sr penetrating into the groundwater, then one would also expect the Sr isotope composition to be more strongly affected towards the isotope signature of the added lime with  $^{87}\text{Sr}/^{86}\text{Sr}$  values around 0.7078. This is clearly not the case as the authors report a  $^{87}\text{Sr}/^{86}\text{Sr}$  value of about 0.7095 for the Karup river head water. A much more likely scenario to explain the [Sr] and  $^{87}\text{Sr}/^{86}\text{Sr}$  changes along the Karup river (supported by the data herein on the soil profile) would be to assign these changes to gradually increasing contributions of Sr derived from deep reaction with relic carbonates along the flow path.

Another Sr mass balance speaking against significant agricultural lime product-based Sr contamination of the surface waters can also be calculated with the data that Thomsen and Andreasen (2019) report for the Vallerbæk tributary to the Karup river (respective catchment area plotted in Fig. 1 for reference). Here, Sr isotope compositions are strongly decreased over a stretch of c. 500 m between position K13 and K4 (their Fig. 4B, C), supposedly where the surface water reaches the groundwater table. Taking their discharge rate of 40 L/s at this transition location, and assuming a farmland-affected catchment area of c. 3 km<sup>2</sup> estimated from their map in Fig. 4B, would consequently translate into a [Sr] in this part of the Vallerbæk brook of around 0.17 mg/L. However, this is a factor of two and a half times higher than what the authors report (0.066 mg/L). Also here, and even more pronouncedly, one would expect the Sr isotope composition in this location of the Vallerbæk brook to be nearly completely biased by the Sr isotope signature of the agricultural lime (i.e.,  $^{87}\text{Sr}/^{86}\text{Sr}$  ~0.7078). This is contrariwise again not reflected by the  $^{87}\text{Sr}/^{86}\text{Sr}$  values of 0.7099 measured in the respective water by Thomsen and Andreasen (2019).

The above mass calculations imply, firstly, that strontium derived from agricultural lime is efficiently retained over decades in the topmost 60 cm of farmland developed on typical glaciogenic outwash sediments and consequently, that this Sr with its specific isotope signature is not transported downward into the respective vadose zone. Secondly, our calculations above on discharge

characteristics within a representative catchment area from within the West Jutland glaciogenic province do not support a scenario whereby Sr from agricultural liming products is, on a yearly basis, efficiently dissolved and effectively transported into the respective vadose zone. [Sr] and Sr isotope compositions of Danish surface run-off, affected by interaction with groundwater recharge from primary and secondary magazines (Gravesen et al., 2010), seem to be controlled by the natural detrital carbonate inventory of the overlying sediments. Our study reveals that very small amounts of relic detrital natural carbonates, still present in the acidic soils typical of moraine and outwash landscapes in western Jutland, are the controlling phases for the isotopic compositions in the respective run-off. This is the reason why significantly replenished water archives, such as creeks, streams and lakes, excerpt homogenized strontium isotope compositions which are biased towards the natural carbonate compositions, as illustrated by the baseline map published by Frei and Frei (2011), redrawn here for reference and illustration purposes in Fig. 6.

#### 4.3. Control of Sr signals by relic detrital carbonates

Data from the soil profile studied herein show an isotopically discernable carbonate endmember in the bioavailable fractions from the agricultural lime carbonate signal (Fig. 2B). Above we interpret that naturally occurring relic detrital carbonates in the sediments have a controlling effect on the isotope compositions of the surface run-off. Our interpretation is compatible with results from a study by Voutchkova et al. (2015), in which it is shown that the distributional pattern of Sr concentrations in Danish groundwaters, including those of central and western Jutland, in fact does reflect the geological/geomorphological outcrop pattern of the overlying sediments. Maps presented by

Voutchkova et al. (2015) (their Fig. 3e,f) reveal a similar distributional pattern of [Sr] in groundwaters as the geomorphological map shown in Fig. 1. This is particularly true for western Jutland, where the waters have expectedly low [Sr], between 0.039 and 0.070 mg/L (Voutchkova et al., 2015). The distributional pattern of low [Sr] waters fits with the distribution of glacial flood plain sediments in Western Jutland (Fig. 1). Since surface run-off and groundwaters are tightly connected with each other, particularly in highly permeable sediments as they occur in periglacial landscapes, the coherence of these maps supports that a natural geogenic system controls the [Sr] in the surface waters. The fact that this concentration-based distributional pattern is not reflected in the distributional pattern of  $^{87}\text{Sr}/^{86}\text{Sr}$  signatures of the surface run-off (i.e., the baseline map published by Frei and Frei (2011); redrawn in Fig. 6), lies therefore in the naturally very low [Sr] of the outwash sediments. These render the vadose system vulnerable to Sr contributions from relict detrital carbonates which bias the  $^{87}\text{Sr}/^{86}\text{Sr}$  towards compositions typical of Late Maastrichtian - Paleocene limestones and chalk which occur widely distributed below the glaciogenic sediment covers in Denmark and which were reworked during the Saale and Weichsel glacier advances. Such detrital carbonates also occur in sediments of the West Jutland glaciogenic province, in some areas constituting up to ~50% of the clastic components in some moraine sediments (Sjørring and Frederiksen, 1980). A natural geogenic (not agricultural lime related) origin of Sr in the surface and groundwaters of Denmark is also supported by the iodine concentrations in them. The distributional pattern of iodine, depicted in the study of Voutchkova et al. (2015) (their Fig. 3a,b) follows that of [Sr]. Voutchkova et al. (2014) found that elevated groundwater-I concentrations originate from Paleocene and Cretaceous limestone/chalk aquifers and attributed a natural source to explain the distribution of this geogenic trace element, very much like for Sr.

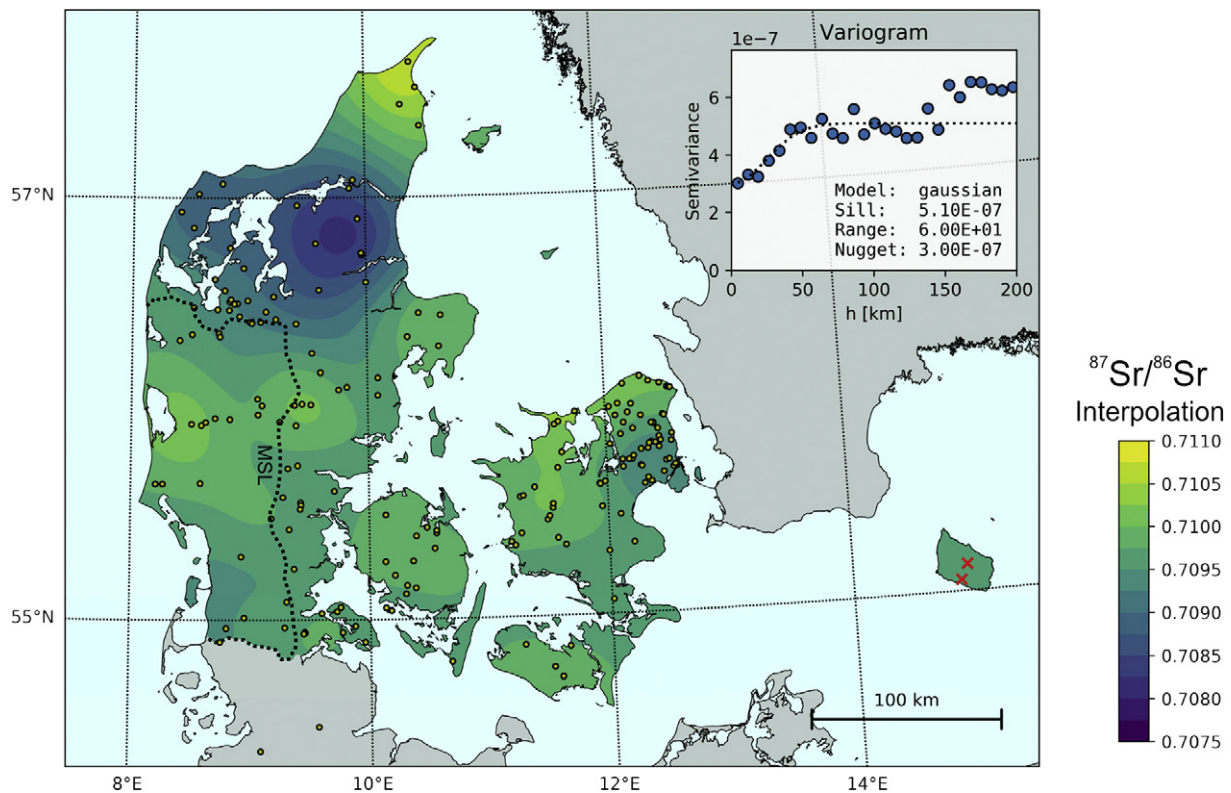


**Fig. 6.** Reference map based on  $^{87}\text{Sr}/^{86}\text{Sr}$  values in surface waters from present - day Denmark (excluding the island of Bornholm). The map is redrawn using the exact data base published by (Frei and Frei, 2011). Surface water sample sites are marked with yellow filled dots. The variogram and variogram parameters (sill, range and nugget) used for the respective  $^{87}\text{Sr}/^{86}\text{Sr}$  interpolation by linear kriging is depicted in the inset. Dotted black line indicates the Main Stationary Line (MSL) which marks the maximum extent of the Scandinavian ice sheet during the last Glaciation (22'000 B.P.).

We also want to point out that, due to the fact that natural detrital carbonates in the acidic parts of glaciogenic sediment profiles have been, and are still, being continuously dissolved,  $^{87}\text{Sr}/^{86}\text{Sr}$  ratios of today's surface run-off likely represent maximum values when for example set in relation to prehistoric periods. This is because one would expect that the relative contribution of Sr with a low  $^{87}\text{Sr}/^{86}\text{Sr}$  signature from these carbonates to the respective vadose zones has decreased over time since the retreat of the glaciers.

In addition, waters analyzed by Thomsen and Andreassen (2019) from springs, creeks and rivers in tunnel valleys and from locations where there is a noticeable increase in water flow rates of surface-run off (such as from the Vallerbæk tributary to the Karup river in the West Jutland glaciogenic province) due to groundwater influx/replenishment, are characterized by significantly higher [Sr] and lower  $^{87}\text{Sr}/^{86}\text{Sr}$  ratios which fall in the range of those published by Frei and Frei (2011) for surface waters from this part of the country. In the view of a groundwater discharge model as presented herein, this implies that large surface water bodies (such as lakes, rivers and large creeks) are not significantly affected by modern agricultural liming and that their Sr isotope signatures are still relevant for modern and prehistoric provenance and migration studies.

#### 4.4. Relevance of surface waters to characterize bioavailable strontium isotope baselines

There seems currently not to be a general consensus regarding the role of drinking water in the strontium intake budget of humans. However, the typical adult human body burden of Sr is 0.3–0.4 g (99% in the skeleton), and the primary exposure sources are drinking water, grains, leafy vegetables, and dairy products (Watts and Howe, 2010). Based on 2 L daily consumption of drinking water with Sr concentrations of 0.34–1.1 mg/L, drinking water contributes 0.7–2 mg/day (Watts and Howe, 2010). Based on these numbers it is conceivable that drinking water might constitute a significant source of Sr in the mass budget of human Sr intake, but not necessarily the sole significant source. The fact that surface run-off is capable of averaging out bioavailable Sr signatures characteristic of a specific area renders this archive relevant and important for provenance and migration studies of humans and animals. While Watts and Howe (2010) note that human Sr intake may be higher in areas where drinking water Sr concentrations are higher, this also applies, in an opposite way, for human Sr intake in areas with low [Sr] in drinking waters. In such areas the drinking water might play a secondary role in the Sr uptake balance of humans and animals. However, Burton and Wright (1995) contributed to the understanding of the complexity of Sr uptake and absorption into human bone and stated that “although bone strontium quantitatively reflects the average dietary Sr/Ca ratio, it is disproportionately sensitive to high-calcium foods”. The importance of strontium in tap water as reflected in human hair has also been advocated by Tipple et al. (2018). Nevertheless, in order for drinking water archives to be relevant in the Sr intake balance of human and animals, it is essential to consider water archives that can serve as realistic and suitable sources of drinking water. This is the case for modern as well as ancient provenance and migration studies. So, for example, we must assume that prehistoric humans likely and preferably drank water from springs, and it is very unlikely that small stagnant water bodies, such as ponds, were chosen for this purpose. Upon these reflections, we re-evaluate the recent surface waters analyzed by Thomsen and Andreassen (2019) from central and western Jutland, considered by these authors as “pristine” sources which they claim to represent archives that are unaffected by modern agricultural lime additions. The elevated radiogenic strontium isotope signatures of surface waters collected from geographically elevated “uplands” (e.g. in ponds) dominated by moraine (till) deposits and outwash plain sediments from the so-called Central and West Jutland glaciogenic provinces (Fig. 1 in Thomsen and Andreassen (2019) between 0.709 and 0.715 are interpreted by them to reflect the true and relevant

bioavailable signature for this part of the country. However, all waters analyzed by Thomsen and Andreassen (2019) and termed “pristine” with high  $^{87}\text{Sr}/^{86}\text{Sr}$  values have [Sr] < 0.07 mg/L, with about half of these samples exhibiting [Sr] < 0.02 mg/L, with values as low as 0.001 mg/L. The low [Sr] of these samples imply a short residence and interaction time with the soil substrate, a feature which would be expected in terranes dominated by highly permeable aquifers. We strongly argue against the claim of Thomsen and Andreassen (2019) that such water bodies with low concentrations have a significant effect on the dietary mass budget of humans, and consequently that these are relevant archives for depicting bioavailable signatures. Using a daily consumption of 2 L water, the contribution of Sr from a drinking water with [Sr] of 0.02 mg/L similar to those waters with elevated  $^{87}\text{Sr}/^{86}\text{Sr}$  signatures analyzed by Thomsen and Andreassen (2019) would imply an insignificant Sr intake proportion of only ~1% if set in relation to an average intake of ~4 mg Sr/day estimated for humans (Watts and Howe, 2010).

#### 4.5. Implications of soil ammonium nitrate leachate signatures for bioavailable fractions

One of the main conclusions from the large and comprehensive data set produced by the GEMAS (Geochemical Mapping of Agricultural Soil; Reimann et al. (2003)) project is that source lithology seems to dominate the soil chemistry. For example, the lead isotope maps produced by the GEMAS consortium (Reimann et al., 2012) show the dominance of the underlying bedrock. However, in this lead isotope study the soil samples were attacked by *aqua regia*, a strong oxidizing acid, which is considered to be representative of bulk mineralogy. This stands in contrast to the weak salt  $\text{NH}_4\text{NO}_3$  extract (also used in this study) which instead better reflects the bioavailable fraction. The  $\text{NH}_4\text{NO}_3$  signal is tentatively also more sensitive to fine-grained atmospheric particle depositions, seaspray and landuse related fertilizer additions, as these influences will dominate in the highly reactive and smallest particle size fraction. Studies of Willmes and co-workers (Willmes et al., 2018; Willmes et al., 2014) used a geo/litho-stratified approach to create a bioavailable  $^{87}\text{Sr}/^{86}\text{Sr}$  map of France for 540 sample locations, using therefore the same  $\text{NH}_4\text{NO}_3$  extraction method for soils as used in the large TRACE project (Voerkelius et al., 2010).  $\text{NH}_4\text{NO}_3$  extractions were also used in the recently published study by Hoogewerff et al. (2019) presenting  $^{87}\text{Sr}/^{86}\text{Sr}$  isotope ratios for ~1200 selected soil samples from adjacent grazing and agricultural topsoils in Europe with the aim to better understand the strontium isotope distribution in the bioavailable fraction of the topsoil and its potential for provenance applications.

Data presented herein on  $\text{NH}_4\text{NO}_3$  extracts from samples of a representative glaciogenic outwash soil profile in the West Jutland glaciogenic province reveals the complexity inherent in the methods to extract bioavailable, labile fractions from soils, and also sheds light on the importance of choosing suitable and relevant soils and extraction methods for this purpose. Here, the extraction of bioavailable Sr from sandy outwash sediments with  $\text{NH}_4\text{NO}_3$  results in more radiogenic  $^{87}\text{Sr}/^{86}\text{Sr}$  values (in the range from 0.7086–0.7104; Table S1, Fig. 3) compared with the compositions measured directly on the pore waters from different soil layers in the respectively studied profile (range from 0.7082–0.7086; Table S1; Figs. 2, 3). However, acetic acid leachates yielding  $^{87}\text{Sr}/^{86}\text{Sr}$  ranging between 0.7072 and 0.7082 (Table S1), designed to specifically attack/dissolve carbonate components in the profile, do show the agricultural lime product imprint in the topmost soil horizons, explicitly revealed by samples B and E which yielded high [Sr] and low  $^{87}\text{Sr}/^{86}\text{Sr}$  signatures of 0.7072–0.7078 (Table S1). Acetic acid leachates from the lower part of the profile instead very closely depict the composition of natural carbonate relicts and approach the  $^{87}\text{Sr}/^{86}\text{Sr}$  signature of 0.70814 (Table S1) of the groundwater sampled at c. 6.6 m depth in the studied profile. It also becomes evident that, in this specific sandy soil profile, the ammonium nitrate leachates “overshoot” the strontium isotope signatures of the pore waters (which are



dominated by Sr from carbonates) in the lower parts of the profile (Figs. 2,3). This implies that very small amounts of adsorbed Sr in these sediments make the bioavailable signature sensitive to contributions from the weathering silicates released by the ammonium nitrate. It also implies that the pore waters measured in the profile are truly characterized by lateral fluxes of water that likely obtained their Sr isotope composition dominantly by partial dissolution of natural relic carbonates in the lower soil horizons of the area that depress the radiogenic isotope signatures of the Sr released from the weathering silicates.

The above implies that ammonium nitrate leaching of sandy sediments, as they occur in the West Jutland glaciogenic province and elsewhere in areas characterized by glacier outwash sediments, is suitable for characterizing relevant bioavailable fractions used for prehistoric and modern provenance studies. In addition, it is not advisable to include sparse surface water bodies from such terranes into constraining bioavailable signature ranges for provenance and migration studies. As mentioned above, neither do the isotope signatures measured in such waters reflect relevant bioavailability, nor do they play an important role in the uptake mass budget of Sr in humans in general.

Last not but least, our study has implications for sampling strategies designed to characterize bioavailable signature ranges of target area in provenance studies based on strontium isotopes. We hypothesize that agriculturally added Sr, including lime, is efficiently concentrated and retained in topsoils, not only in glaciogenic outwash terrains of Northern Europe where podzols dominate, but also in other farmed areas elsewhere characterized by other soil types, particularly by calcisols, cambisols and chernozems with defined organic-rich top horizons which occur widespread at least on the European continent. If sampling of such agriculturally affected soils cannot be circumvented, it is advisable to collect soil samples below the organic-rich zone as we suspect that, as shown by our study herein, Sr effectively is adsorbed by organic material and exogenous Sr therefore would significantly affect the bioavailable, geo-pedogenic-sourced natural Sr fraction leached from these soils for provenance purposes. We however note here that a recently published study by Hoogewerff et al. (2019) comparing  $\text{NH}_4\text{NO}_3$  soil extracts of c. 1200 topsoils (from 0 to 20 cm depth) of respective agricultural farmland. In their study, nearby grassland samples from all over Europe did not significantly discriminate the  $^{87}\text{Sr}/^{86}\text{Sr}$  signatures between the two groups. The difference in  $^{87}\text{Sr}/^{86}\text{Sr}$  means between the agricultural farmland sample extracts and the extracts from grassland soil sites is 0.0009 and between the medians just 0.0003, while there is slight difference of 0.0011 in the standard deviations defined by the two data sets (Hoogewerff et al., 2019).

As vegetation is increasingly used as a potential archive from which bioavailable signatures can be extracted, it would make sense to sample plants with root system deep enough to penetrate beyond the organic-rich top soils of respective terranes. Bushes seem to be better suited than surface plants such as grass, heather etc. for this purpose. More detailed studies are however necessary to investigate the effects of exogenous Sr on potentially interesting alternative proxy archives to surface run-off, for the construction of adequate and realistic baselines and isoscapes used for provenancing.

## 5. Conclusions

Our detailed study of a representative cored soil profile characterized by sandy glaciogenic outwash sediments in the West Jutland glaciogenic province comes as a response to the recently published article by Thomsen and Andreassen (2019) in which these authors convey a strong criticism towards the use of strontium isotope signatures of surface-run-off in such terranes, for the definition of bioavailable signatures, with far reaching implications for existing and futures provenance and migration studies of prehistoric humans and animals. We here show that agricultural liming of soils in areas dominated by siliciclastic outwash overburden does not influence the strontium isotope

composition of the vadose zone, and that the transfer of cations (including  $\text{Sr}^{2+}$ ) from agricultural lime products added to the topsoils is efficiently inhibited by an alkalinity barrier near the surface.

Down-log mixing relationships between inverse strontium concentrations and  $^{87}\text{Sr}/^{86}\text{Sr}$  signatures in ammonium nitrate leachates of the core samples studied reveal that the top 60 cm of the soil studied is strongly affected by lime product addition. Conversely, released strontium from the samples below this horizon can be explained by a well-defined two component system, with dominant strontium derived from relic, naturally occurring Late Maastrichtian-Early Danian limestone components and a radiogenic component derived from the weathering of siliciclastic material.

The increasing [Sr] and decreasing  $^{87}\text{Sr}/^{86}\text{Sr}$  values in many brooks and rivers from the West Jutland glaciogenic province could result from discharging deep flow groundwater paths carrying a Sr imprint from detrital relic carbonates and need therefore not be associated to the change in land use along the respective brooks and rivers. In this view, existing surface-water based reference isoscapes and respective reference maps in recently glaciated farmed areas are still valid.

We show that pore waters and the groundwaters are dominated by strontium derived from naturally occurring relic carbonate components in these otherwise termed “low to noncalcareous” sediments, and that the presence of even very small amounts of such relic detrital carbonates in the soil profiles are sufficient to bias the  $^{87}\text{Sr}/^{86}\text{Sr}$  ratios measured in the respective pore waters and in ammonium nitrate leachates designed to recover bioavailable strontium isotope signatures from the substrates. This is one of the major reasons why surface-water based strontium isotope reference maps, such as published by Frei and Frei (2011) for Denmark (excluding the island of Bornholm) show a rather homogenous distribution of strontium isotopes including the West Jutland glaciogenic province. The strong interaction between surface-water run-off and groundwater in such terranes predicts that such a homogenous strontium isotope distribution is also found in respective groundwaters in Denmark.

Our results also imply that sparse surface waters with very low [Sr] in otherwise very permeable sediments typical of glaciogenic outwash terranes are not suitable for the characterization of relevant bioavailable signatures used for provenance and migration studies.

Finally, if drinking water is to be considered a significant contributor to a daily Sr intake of a human, the strontium concentrations of such waters should be high enough to be able to contribute with a significant proportion to an average daily strontium intake. It is these characteristics that are not met by most of the surface waters sampled by Thomsen and Andreassen (2019) from upland areas in the West Jutland glaciogenic province, and we argue against strontium isotope signatures measured on them to be relevant for prehistoric and modern provenance studies.

## Acknowledgments

General: We thank Cristina Nora Jensen for help with sample preparations and ion chromatographic separations, and Toby Leeper for always keeping the mass spectrometers at IGN in perfect running conditions. Pernille Ladegaard-Pedersen contributed with relevant discussions and literature search. We also thank Dieke Postma and Rasmus Jacobsen, both affiliated to GEUS, for allowing us to use the data from the  $\text{CO}_2$ -GS field site. Trygvi Bech Árting helped in computing the map in Fig. 6. Karsten Høgh Jensen is thanked for facilitating the collaboration. We are thankful to four anonymous reviewers who provided insightful and constructive comments and suggestions which improved our final manuscript.

## Funding

RF is thankful to Carlsberg Foundation's support for new analytical facilities (mass spectrometers), through grants 2012-01-071 and



CF17-102. KMF acknowledges support by the Carlsberg Foundation through the project entitled "Tales of Bronze Age Women" CF-15 0878 and through the "Semper Ardens" research CF18-0005 (Tales of Bronze Age People). The CO<sub>2</sub>-GS field site was funded by a grant of the Danish Council for Strategic Research (DSF-09-067234).

## Author contributions

RF designed the project, performed the mass spectrometrical analyses, and wrote the main part of the manuscript. KMF helped with the design of the project and with compiling relevant literature. SJ conducted and led the fieldwork, and designed and performed the core sampling. KMF and SJ contributed with writing of the manuscript.

## Declaration of competing interests

The authors acknowledge herewith that they have no conflict of interest.

## Appendix A. Supplementary data

Supplementary data to this article can be found online at <https://doi.org/10.1016/j.scitotenv.2019.135710>.

## References

- Bentley, R.A., 2006. Strontium isotopes from the earth to the archaeological skeleton: a review. *J. Archaeol. Method Theory* 13, 135–187.
- Böhlke, J.K., Wanty, R., Tuttle, M., Delin, G., Landon, M., 2002. Denitrification in the recharge area and discharge area of a transient agricultural nitrate plume in a glacial outwash sand aquifer, Minnesota. *Water Resour. Res.* 38, 10–1–10–26.
- Boyer, A., Ning, P., Killey, D., Klukas, M., Rowan, D., Simpson, A.J., et al., 2018. Strontium adsorption and desorption in wetlands: role of organic matter functional groups and environmental implications. *Water Res.* 133, 27–36.
- Burton, J.H., Wright, L.E., 1995. Nonlinearity in the relationship between bone Sr/Ca and diet: Paleodietary implications. *Am. J. Phys. Anthropol.* 96, 273–282.
- Evans, J.A., Montgomery, J., Wildman, G., Bouton, N., 2010. Spatial variations in biosphere <sup>87</sup>Sr/<sup>86</sup>Sr in Britain. *J. Geol. Soc.* 167, 1–4.
- Flockhart, D.T.T., Kyser, T.K., Chipley, D., Miller, N.G., Norris, D.R., 2015. Experimental evidence shows no fractionation of strontium isotopes (<sup>87</sup>Sr/<sup>86</sup>Sr) among soil, plants, and herbivores: implications for tracking wildlife and forensic science. *Isot. Environ. Health Stud.* 51, 372–381.
- Frei, R., Frei, K.M., 2002. A multi-isotopic and trace element investigation of the cretaceous-tertiary boundary layer at Stevns Klint, Denmark - inferences for the origin and nature of siderophile and lithophile element geochemical anomalies. *Earth Planet. Sci. Lett.* 203, 691–708.
- Frei, K.M., Frei, R., 2011. The geographic distribution of strontium isotopes in Danish surface waters - a base for provenance studies in archaeology, hydrology and agriculture. *Appl. Geochem.* 26, 325–340.
- Frei, K.M., Price, T.D., 2012. Strontium isotopes and human mobility in prehistoric Denmark. *Archaeol. Anthropol. Sci.* 4, 103–114.
- Frei, K.M., Mannering, U., Kristiansen, K., Allentoft, M.E., Wilson, A.S., Skals, I., et al., 2015. Tracing the dynamic life story of a bronze age female. *Sci. Rep.* 5.
- Frei, K.M., Villa, C., Jorkov, M.L., Allentoft, M.E., Kaul, F., Ethelberg, P., et al., 2017. A matter of months: high precision migration chronology of a Bronze Age female. *PLoS One* 12.
- Friberg, R., 1996. The landscape below the Tinglev outwash plain: a reconstruction. *Bull. Geol. Soc. Den.* 43, 34–40.
- Gilleaudeau, G.J., Voegelin, A.R., Thibault, N., Moreau, J., Ullmann, C.V., Kläbe, R.M., et al., 2018. Stable isotope records across the Cretaceous-Paleogene transition, Stevns Klint, Denmark: new insights from the chromium isotope system. *Geochim. Cosmochim. Acta* 235, 305–332.
- Gravesen, P., Nilsson, B., Pedersen, S.A.S., Binderup, M., Lai, T., 2010. Low- and intermediate level radioactive waste from Risø, Denmark. Location Studies for Potential Disposal Areas. 123. Denmark of Grønlands Geologiske Undersøgelse Rapport, p. 78 Report no 2.
- Greve, M.H., Kheir, R.B., Greve, M.B., Böcher, P.K., 2012. Using digital elevation models as an environmental predictor for soil clay contents. *Soil Sci. Soc. Am. J.* 76, 2116–2127.
- Hansen, B.K., Postma, D., 1995. Acidification, buffering, and salt effects in the unsaturated zone of a sandy aquifer, Klosterhede, Denmark. *Water Resour. Res.* 31, 2795–2809.
- Hobson, K.A., 1999. Tracing origins and migration of wildlife using stable isotopes: a review. *Oecologia* 120, 314–326.
- Hoogewerff, J.A., Reimann, C., Ueckermann, H., Frei, R., Frei, K.M., van Aswegen, T., et al., 2019. Bioavailable <sup>87</sup>Sr/<sup>86</sup>Sr in European soils: a baseline for provenancing studies. *Sci. Total Environ.* 672, 1033–1044.
- Jessen, S., Postma, D., Jakobsen, R., Looms, M.C., Larsen, F., 2014. Inhibition of carbon transfer across the vadose zone by 20th century acid rain. EGU General Assembly. EGU2014-6340, Vienna.
- Kystol, J., Larsen, L.M., 1999. Analytical procedures in the rock geochemical laboratory of the Geological Survey of Denmark and Greenland. *Geol. Greenl. Surv. Bull.* 184, 59–62.
- Lindsay, W.L., 1979. *Chemical Equilibrium in Soils*. John Wiley & Sons, New York.
- Maurer, A.F., Galer, S.J.G., Knipper, C., Beierlein, L., Nunn, E.V., Peters, D., et al., 2012. Bioavailable Sr-87/Sr-86 in different environmental samples - effects of anthropogenic contamination and implications for isoscapes in past migration studies. *Sci. Total Environ.* 433, 216–229.
- van der Merwe, N.J., Lee-Thorp, J.A., Thackeray, J.F., Hall-Martin, A., Kruger, F.J., Coetzee, H., et al., 1990. Source-area determination of elephant ivory by isotopic analysis. *Nature* 346, 744–746.
- Montgomery, J., 2010. Passports from the past: investigating human dispersals using strontium isotope analysis of tooth enamel. *Ann. Hum. Biol.* 37, 325–346.
- Müller, W., Fricke, H., Halliday, A.N., McCulloch, M.T., Wartho, J.-A., 2003. Origin and migration of the alpine iceman. *Science* 302, 862–866.
- Newton, P.N., Fernández, F.M., Plançon, A., Mildenhall, D.C., Green, M.D., Ziyong, L., et al., 2008. A collaborative epidemiological investigation into the criminal fake Artesunate trade in South East Asia. *PLoS Med.* 5, e32.
- Odgaard, B.V., Rasmussen, P., 2000. Origin and temporal development of macro-scale vegetation patterns in the cultural landscape of Denmark. *J. Ecol.* 88, 733–748.
- Postma, D., Boesen, C., Kristiansen, H., Larsen, F., 1991. Nitrate reduction in an unconfined sandy aquifer: water chemistry, reduction processes, and geochemical modeling. *Water Resour. Res.* 27, 2027–2045.
- Price, T.D., Burton, J.H., Bentley, R.A., 2002. The characterization of biologically available strontium isotope ratios for the study of prehistoric migration. *Archaeometry* 44, 117–135.
- Reardon, E.J., Allison, G.B., Fritz, P., 1979. Seasonal chemical and isotopic variations of soil CO<sub>2</sub> at Trout Creek, Ontario. In: Back, W., Stephenson, D.A. (Eds.), *Developments in Water Science* 12. Elsevier, pp. 355–371.
- Reimann, C., Birke, M., Demetriades, A., Filzmoser, P., O'Connor, E.A., 2003. *Agricultural Soils in Northern Europe: A Geochemical Atlas*. Heft 5. Geologisches Jahrbuch, Sonderhefte Reihe D, p. 279.
- Reimann, C., Flem, B., Fabian, K., Birke, M., Ladenberger, A., Négrel, P., et al., 2012. Lead and lead isotopes in agricultural soils of Europe - the continental perspective. *Appl. Geochem.* 27, 532–542.
- Robertson, W.D., Russell, B.M., Cherry, J.A., 1996. Attenuation of nitrate in aquitard sediments of southern Ontario. *J. Hydrol.* 180, 267–281.
- Sjørring, S., Frederiksen, J., 1980. Glacialstratigrafiske observationer i de vestjyske bakkeøer. *Dansk Geologiske Forening Årsskrift for 1979*, pp. 63–77.
- Thaysen, E.M., Jessen, S., Postma, D., Jakobsen, R., Jacques, D., Ambus, P., et al., 2014. Effects of lime and concrete waste on vadose zone carbon cycling. *Vadose Zone J.* 13.
- Thirlwall, M.F., 1991. Long-term reproducibility of multicollector Sr and Nd isotope ratio analysis. *Chemical Geology: Isotope Geoscience section* 94, 85–104.
- Thomsen, E., Andreassen, R., 2019. Agricultural lime disturbs natural strontium isotope variations: implications for provenance and migration studies. *Sci. Adv.* 5, eaav8083.
- Tipple, B.J., Valenzuela, L.O., Ehleringer, J.R., 2018. Strontium isotope ratios of human hair record intra-city variations in tap water source. *Sci. Rep.* 8, 3334.
- Voerkelius, S., Lorenz, G.D., Rummel, S., Quélet, C.R., Heiss, G., Baxter, M., et al., 2010. Strontium isotopic signatures of natural mineral waters, the reference to a simple geological map and its potential for authentication of food. *Food Chem.* 118, 933–940.
- Voutchkova, D.D., Kristiansen, S.M., Hansen, B., Ernsten, V., Sørensen, B.L., Esbensen, K.H., 2014. Iodine concentrations in Danish groundwater: historical data assessment 1933–2011. *Environ. Geochem. Health* 36, 1151–1164.
- Voutchkova, D.D., Schullehner, J., Knudsen, N.N., Jørgensen, L.F., Ersbøll, A.K., Kristiansen, S.M., et al., 2015. Exposure to selected geogenic trace elements (Li, I, and Sr) from drinking water in Denmark. *Geosciences* 5, 45–66.
- Watts, P., Howe, P., 2010. Strontium and strontium compounds. *Concise International Chemical Assessment Document*. 77. World Health Organization (WHO), Geneva, Switzerland, pp. 1–67.
- West, J.B., Hurley, J.M., Dudás, F., Ehleringer, J.R., 2009. The stable isotope ratios of marijuana. II. Strontium isotopes relate to geographic origin. *J. Forensic Sci.* 54, 1261–1269.
- Willmes, M., McMorrow, L., Kinsley, L., Armstrong, R., Aubert, M., Eggins, S., et al., 2014. The IRHUM (isotopic reconstruction of human migration) database & bioavailable strontium isotope ratios for geochemical fingerprinting in France. *Earth Syst. Sci. Data* 6, 117–122.
- Willmes, M., Bataille, C.P., James, H.F., Moffat, I., McMorrow, L., Kinsley, L., et al., 2018. Mapping of bioavailable strontium isotope ratios in France for archaeological provenance studies. *Appl. Geochem.* 90, 75–86.